Senior Thesis: Nonthermal Emission from Black Hole Accretion Flows

John McCann

Department of Physics, University of Illinois at Urbana–Champaign, 1110 W. Green Street, Urbana, IL 61801

22nd of November, 2013

Contents

Abstract

We describe an approximate fitting formula of the radiative transfer coefficients for synchrotron emission from a nonthermal electron distribution function. Quasi-analytic solutions for the coefficients have previous existed; however, their calculations proved too computationally expensive for direct use in radiative transfer calculations. With the approximate fitting formula implementation, we used a conservative numerical scheme for general relativistic magnetohydrodynamics to simulate accreting supermassive Kerr black holes. Simulated data is then analyzed using ray tracing methods and compare with observational data from Sagittarius A* at the sub millimeter range. We found that the simulations are able to account for the near-infrared emission with a nonthermal component in the synchrotron emission. The resulting model will provide greater insight to the physical process of supermassive black holes, allowing for the testing of strong gravity theories.

Abstract

The work presented details computer simulations of the emission from massive spinning black holes, such as the one found at the center of our Milky Way galaxy. Prior models have either been unsuccessful or poorly motivated in explaining emission seen in observation at higher energies, while well motivated process to explain the high energy emission have previous been too computationally intensive to be carried out. However, we have found a computationally cheap method to perform these calculations with excellent agreement to the intensive method. Using the new method we modify a previous model, adding new particle constituents, differing from the old particles in their physical properties, to the the black hole's environment. The addition of the new constituents has lead to agreement between the observational data and our model, while being properly motivated.

1 INTRODUCTION

Sagittarius A* (Sgr A*) is part of the Sagittarius A system located at the center of Milky Way. Sgr A* is a bright compact radio source, home to a supermassive black hole, which is of interest since it is currently the closest known supermassive black hole to Earth. Moreover, Sgr A* subtends the largest portion of our sky out of all known black holes, and will allow for the greatest observational resolution of black holes. Studying Sgr A* will allow us to test theories of strong gravity, which have remained poorly tested.

Of particular interest to this thesis, is emission from a nonthermal component in the accretion disc around Sgr A*. We will explore the idea of using a nonthermal component, emitting via synchrotron radiation, to explain the infrared observations of Sgr A* [1]. While a variety of other processes could give rise to infrared emission [2], we argue that the polarization of the infrared emission strongly suggest that the underlaying process is synchrotron radiation.

The work presented, builds off an unpublished ray tracing model, written by Dr. Charles F. Gammie of the University of Illinois at Urbana-Champaign, that has been able to account for emission in the centimeter range. The previous model used only a thermal component of the electron distribution for synchrotron emission; however, the model failed to produce adequate emission in the infrared region. Other work has also been done to try and account for infrared emission with Compton scattering [3]. However, the Compton scattering model has issues explaining the polarization seen in the observational data, while a defining characteristic of synchrotron radiation is its highly polarized emission.

We use a conservative numerical scheme for general relativistic magnetohydrodynamics (GRMHD) to simulate an accreting black hole [4] [5]. The model uses primitive and conserved variables to progress through time in the simulation. The simulated data is then fed into a ray tracing code, which uses radiative transfer to calculate the emission an observed would see a certain distance and angle away from the black hole. Using parameters to describe best Sgr A*, we can compare the simulated data to observations.

In § 2 the model used for the simulation of the black hole and the ray tracing model is described. The parameters of the model and a discussion on synchrotron radiation is also found. In § 3 we present the results obtained form the simulations; including are spectrums and light curves along with the approximate fitting formula we found. In § 4 we discuss implications of the results. In § 5 and § 6, a conclusion of the findings is presented along with future work relating to the project.

2 METHODS

2.1 Simulation data

For our models, a black hole with an accretion disc is simulated in 2D. GRMHD simulations of the accretion disk are then used to evolve the disk in time. Specifically, the GRMHD code used is a 2D version of HARM [4], dubbed iHARM2D. Simulations by iHARM2D are carried out by numerically solving the hyperbolic partial differential GRMHD equation of motion using conservative, shock-capturing techniques. These calculations are done for a stationary black hole in the Kerr–Schild coordinate system.

In these simulations a torus is seeded around a black hole with an initial density, poloidal magnetic field and maximum pressure at 12 GM/c [1]. Various physical parameters of the torus are tracked such as the electron density, 4-magnetic field, 4-velocity and internal energy. Our simulations typically run for 2000 GM/c^3, and the parameters are recorded in dump files every 2 GM/c^3.

The simulation takes place from just inside the event horizon to 40 GM/c. For a Kerr black hole, the event horizon distance, in units of M, is given by

$$r_{event} = \frac{GM}{c^2} + \sqrt{\left(\frac{GM}{c^2}\right)^2 - \left(\frac{J}{Mc}\right)^2}, \tag{1}$$

where J is the angular momentum of the spinning black hole.

Boyer-Lindquist coordinates are used in the simulation; however, the resolution is compacted when radial close to the black hole and for polar angles near the equator. The two resolution coordinates are X_1 and X_2, which are related to the standard polar coordinates by

$$r = e^{X_1}, \tag{2}$$

$$\theta = \pi X_2 + \frac{1 - h_{slope}}{2} \sin\left(2\pi X_2\right), \tag{3}$$

where h_{slope} is a parameter, between 0 and 1, used to alter the compression of the X_2 coordinate near the equator. For this thesis, a typical iHARM2D run is done at 256×256 resolution in (X_1, X_2).

HARM is capable of producing maps of various parameters of interest, as shown in Figure 1.

[1] G is Newton's gravitational constant, M is the mass of the black hole, c is the speed of light in vacuum. When choosing to use units where $G = c = 1$, M can represents mass, distance, or time.

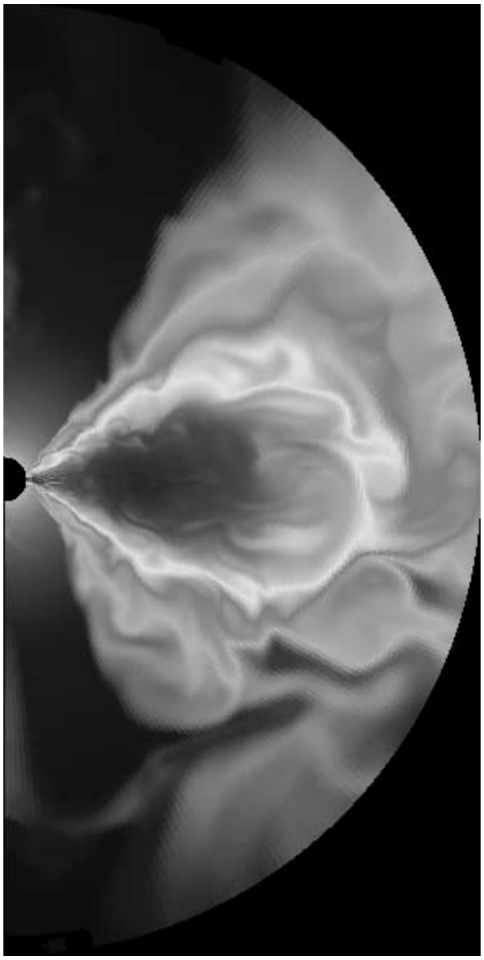

Figure 1: Shown is a mapping produce by HARM of the density field for a Kerr black hole with $J/Mc = 0.5$ at $t = 2000$ GM/c. A greyscale is used to represent the electron density with black being the least dense. We note that the black hole is the black circle in the center left margin, and the denser areas are where the accretion disk is found. The resolution of the run is 300×300 [4].

2.2 Ray tracing

From iHARM2D's simulated data, relativistic radiative transfer can be performed. Our work used a program called ibothros2d to trace light rays backwards in time along their null geodesics to the black hole. When the ray enters the accretion disc, the radiative transfer equation is solved to determine the ray's behavior. The

radiative transfer equation is

$$I_\nu(s) = I_\nu(s_0)e^{-\tau_\nu(s,s_0)} + \int_{s_0}^{s} j_\nu(s')e^{\tau_\nu(s',s)}\mathrm{d}s', \tag{4}$$

where s is the position, I_ν is the specific intensity, $\tau_\nu(s_1, s_2) \equiv \int_{s_1}^{s_2} \alpha_\nu(s)\mathrm{d}s$, is the optical depth, α_ν is the absorptivity, and j_ν is the emissivity. Once the calculation is complete, the intensity seen by the observer for that geodesic is obtained and can be used as the flux for that pixel's steradian.

The program ibothros2d must be given the frequency of the ray, the X_2 coordinate from which the observer sits, and a normalizing mass, which is related to the black hole's accretion rate. Additionally, to get measurements in cgs, the mass of the black hole and distance to the source must be specified. With the solved flux from each zone, several analyses can be run from ibothros2d. These include light curves, spectra and movies of the evolution of the accretion disc.

2.3 Synchrotron emission

To solve the relativistic radiative transfer equation, we first calculate the absorptivity and emissivity of the accretion disk. In our model we assume that synchrotron radiation is the dominate source of radiation from the accretion disc. In thermal equilibrium the emission and absorption coefficients depend on only density and temperature, and are related by

$$j_\nu = \alpha_\nu B_\nu(T), \tag{5}$$

where $B_\nu(T)$ is spectral radiance determined by Planck's law.

For a thermal electron distribution function, with an electron temperature much greater than 1 and a frequency much greater than the synchrotron frequency, the emissivity coefficient is given by [1]

$$j_\nu \approx n_e \frac{\sqrt{2}\pi e^2 \nu_s}{6\Theta_e^3 c} X \exp\left(-X^{1/3}\right), \tag{6}$$

where n_e is the electron density, Θ_e is the electron temperature, $\nu_s \equiv (2/9)\nu_c \Theta_e^2 \sin\theta$, the synchrotron frequency, $\nu_c \equiv \frac{eB}{2\pi m_e c}$, the cyclotron frequency, and $X \equiv \nu/\nu_s$. From the emissivity we can then calculate the absorptivity by (5), and then use the absorptivity and spectral radiance to calculate the intensity.

In a nonthermal electron distribution function, the relation given by (5), no longer holds. Therefore, the emissivity and absorptivity coefficients must both be calculated

in order to solve the radiative transfer equation. Our model uses nonthermal electrons having a distribution following a power law in electron energy of constant index p between γ_{min} and γ_{max}, the minimum and maximum Lorentz factors of the nonthermal electrons. In our model the power law electrons and nonthermal electrons are equivalent and used interchangeably. The nonthermal synchrotron emissivity j_{pl} and absorptivity α_{pl} coefficients for these nonthermal electrons are given by [1]

$$j_{pl} = n_e^{NT} \left(\frac{e^2 \, \nu_c}{c} \right) \frac{3^{p/2} \, (p-1) \sin\theta}{2 \, (p+1) \left(\gamma_{min}^{1-p} - \gamma_{max}^{1-p} \right)} \times \Gamma \left(\frac{3p-1}{12} \right) \Gamma \left(\frac{3p+19}{12} \right) \left(\frac{\nu}{\nu_c \sin\theta} \right)^{-(p-1)/2}, \tag{7}$$

$$\alpha_{pl} = n_e^{NT} \left(\frac{e^2}{\nu \, m_e \, c} \right) \frac{3^{(p+1)/2} \, (p-1)}{4 \left(\gamma_{min}^{1-p} - \gamma_{max}^{1-p} \right)} \times \Gamma \left(\frac{3p+2}{12} \right) \Gamma \left(\frac{3p+22}{12} \right) \left(\frac{\nu}{\nu_c \sin\left(\theta\right)} \right)^{-(p+2)/2}, \tag{8}$$

where n_e^{NT} is the number density of the nonthermal electrons.

Two models were used to relate the ratio of nonthermal electrons to thermal electrons. The first model was a fixed fraction of the density comprising nonthermal electrons. A second model uses a fixed energy ratio between the nonthermal and thermal components. The relationship is as follows [6]

$$N_{pl} = \eta a(\Theta_e) \Theta_e (p-2) N_{th}, \tag{9}$$

where N_{pl} is the total number of power law electrons, N_{th} is the total number of thermal electrons, η is the ratio between the nonthermal and thermal energy and $a(\Theta_e)$ is a relativistic factor depending on electron temperature. Analytically $a(\Theta_e)$ is given by

$$a(\Theta_e) \equiv \frac{1}{\Theta_e} \left[\frac{3K_3(1/\Theta_e) + K_1(1/\Theta_e)}{4K_2(1/\Theta_e)} - 1 \right], \tag{10}$$

where K_n are the modified Bessel functions of order n. However, $a(\Theta_e)$ can be approximated with an absolute relative error of 2% by [7]

$$a(\Theta_e) = \frac{6 + 15\Theta_e}{3 + 5\Theta_e}. \tag{11}$$

2.4 Modeling nonthermal electrons with a power law distribution

We assume that the energy density, u, of the nonthermal component, modeled by a power law, is related to the thermal component by some factor η. That is to say that, $u_{pl} = \eta\, u_{th}$, where u_{pl} and u_{th} are the energy densities for the power law and thermal components respectively. For a relativistic electron distribution the energy density is given by

$$u = \int \mathrm{d}\gamma (1-\gamma) m_e c^2 \frac{\mathrm{d}n}{\mathrm{d}\gamma}. \tag{12}$$

For a power law electron distribution, the derivative of the electron density with respects to the Lorentz factor is, $\frac{\mathrm{d}n}{\mathrm{d}\gamma} = N_{pl}(p-1)\gamma^{-p}$, where N_{pl} is the total number of power law electrons, and p is the power law index. This electron density per Lorentz factor is chosen, since it has the behavior that when integrated over gamma (from 1 to ∞), for a $p \geq 1$, it gives N_{pl}. Inserting the power law $\frac{\mathrm{d}n}{\mathrm{d}\gamma}$ into Equation (12), and integrating over all physical γ's, we get that

$$\begin{aligned} u_{pl} &= \int_1^\infty \mathrm{d}\gamma (\gamma - 1) m_e c^2 N_{pl} (p-1) \gamma^{-p} \\ &= N_{pl} m_e c^2 (p-1) \left[\int_1^\infty \mathrm{d}\gamma\, \gamma^{-p+1} - \int_1^\infty \mathrm{d}\gamma\, \gamma^{-p} \right] \\ &= N_{pl} m_e c^2 (p-1) \left[\frac{1}{p-2} \gamma^{-p+2} \Big|_\infty^1 - \frac{1}{p-1} \gamma^{p-1} \Big|_\infty^1 \right], \end{aligned}$$

which converges only if $p \geq 2$. Letting $p \geq 2$ then

$$u_{pl} = \frac{N_{pl} m_e c^2}{p-2}. \tag{13}$$

From 'The Quantum Statistics' chapter in the book "An Introduction to the Study of Stellar Structure" written by Chandrasekhar, we can follow his derivation to see that for the thermal component

$$u_{th} = N_{th} a(\Theta_e) \Theta_e m_e c^2, \tag{14}$$

where $a(\Theta_e)$ is given by Equation (10).

Using the assumed relationship between the nonthermal and thermal energy and substituting in Equations (13) and (14), we get

$$N_{pl} = \eta a\left(\Theta_e\right) \Theta_e \left(p-2\right) N_{th}, \tag{15}$$

which is Equation (9).

2.5 Model parameters

The model parameters are the parameters which define the radiative model. Parameters are chosen to best model Sgr A*. The mass of black hole is $4.5 \times 10^6\ M_\odot$ and the distance to source is 8.3×10^3 parsecs. The spin of the black hole is fixed at $a/M = 0.9375$, the ion–electron temperature Θ_i/Θ_e for the disk is set to 3 [8], accretion rate $\dot{M}$ is taken to be 6×10^{18} grams·sec^{-1}, minimum allowed Θ_e is 0.3, maximum allowed Θ_e is 100, and γ_{min}, γ_{max} are set to 1 and 1000 respectively. The power law index p and fraction of energy in the nonthermal component of the distribution are left as a free parameters.

3 RESULTS

3.1 Simulation agreement

From the two family of codes, Bothros and GrMonty, excellent agreement has been found between their output. The two codes use separate models to calculate the spectra from from the accretion flow. The significance of the agreement is that we have two independent simulations, using different methods, that generate the same results.

GrMonty uses a Monte Carlo method, which randomly samples regions of the grid and calculates the flux. Bothros, on the other hand, uses ray-tracing methods and calculates the emissivity and absorptivity of the plasma along the geodesics of the photon. Both of these simulations then output spectra of the specific luminosity of the emission.

For ibothros2d, we use a $X_2 = 0.425$, which can be related to the observer's angle from (3). GrMonty, on the other hand, breaks the polar grid from 0 to π up into ten bins by choice. The spectra produced from each bin will best represent the flux observed at the mean polar value for that bin. Therefore, the spectrum generated from the 8^{th} bin of GrMonty, mean polar value of 67.5°, will most closely match the spectrum from ibothros2d x_2 value of 0.425, or polar value of 67.4°.

Since ibothros2d does not account for Compton scattering in its model, this process is turned off in GrMonty to test their agreement. Equally important is that ibothros2d's electron distribution be completely thermal, since GrMonty does not simulate nonthermal emission. The parameters of the black hole being simulated must also agree between the codes; mass of black hole $4.5 \times 10^6\ M_\odot$, distance to source 8.3×10^3 parsecs, $\dot{M}$ is 6×10^{18} grams·sec^{-1} and a $\Theta_i : \Theta_e$ of 3. The comparison using the described parameters is shown in Figure 2.

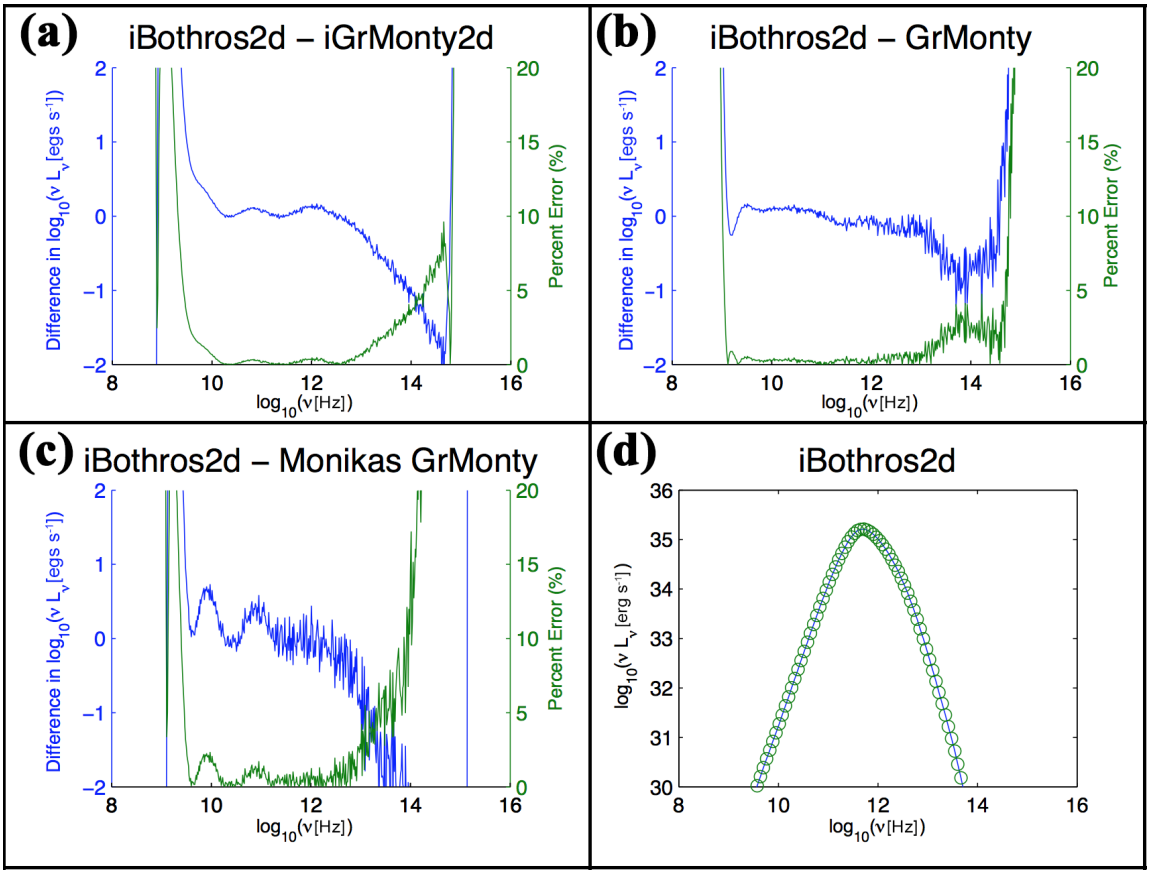

Figure 2: Plots of the agreement between ibothros2d and three different Monte Carlo codes are shown. Plot (a), (b) and (c) show the differences between the ibothros2d and three different Monte Carlo codes. Shown in each of these graphs are the differences between the simulation in blue, and the percent difference in green. Plot (d) shows the simulation produced for ibothros2d.

3.2 Power law distribution

To account for emission from the infrared region of the observational spectrum, we used synchrotron emission from a nonthermal electron distribution. These highly energetic electrons are capable of emitting photons at higher frequencies and account for the emission in the infrared. The reason for using synchrotron radiation instead of other processes, such as Compton scattering, is the highly polarized emission from observational data. Synchrotron radiation best accounts for the highly polarized observed emission, and at such high energies, a nonthermal component is necessary.

Currently, the physical process responsible for the generation of nonthermal particles around black holes is not known.

Implementing this model into the code required altering the electron distribution. The two models used are discussed in Section 2.3. We have chosen the what we believe to be the more physically relevant model with a fixed energy ratio between the two components of the electron distribution, i.e., the fixed energy ratio is modeled by

$$N_{pl} = \eta a\left(\Theta_e\right)\Theta_e\left(p-2\right)N_{th}. \tag{16}$$

With the fixed energy fraction implementation for a power law distribution, the spectra are produced as shown in Figure 3. Note that the power law tail continues indefinitely, and will producing a large amount of infinite energy photons. These infinite energy photons are unphysical and will require adjustments to the model; however, we can see that emission in the infrared region is obtained. The power law distribution contributes to the entire spectrum; such as the small, low-frequency shoulder. However, the low-frequency shoulder is not the main focus of this discussion, since it is currently observationally irrelevant.

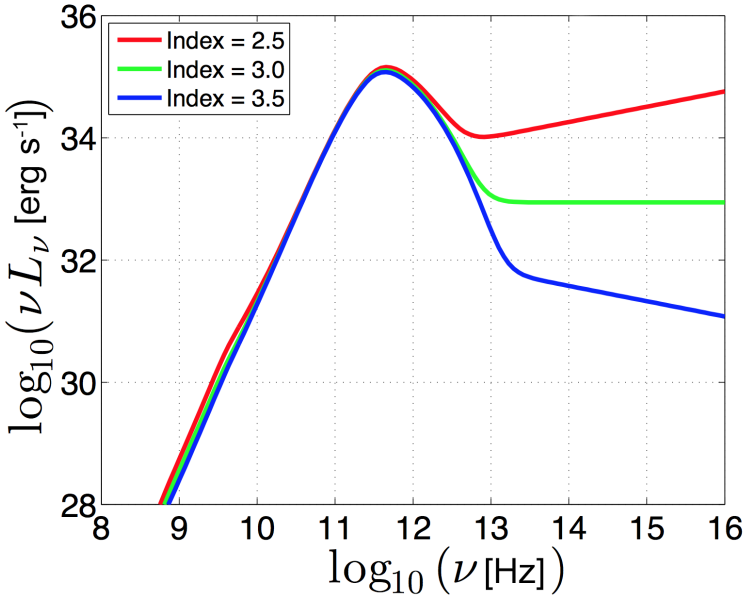

Figure 3: A spectrum of an accreting black hole having a nonthermal component to the electron distribution function modeled using a power law. The power law index is left as a parameter that can be used to change the shape of the power law tail, which currently will extended to infinity leading to unphysical product of infinity energy photons.

3.3 Approximate fitting formula

For a computationally cheap method of computing the nonthermal coefficients of emissivity and absorptivity, a power law distribution with an approximate fitting formula is used. The fit was chosen to depend on the relevant parameters that effect the emission coefficients: B the magnetic field strength, θ the angle between the photon wave vector and the magnetic field line, ν the emitted photon frequency, and γ_{cutoff} the maximum Lorentz factor of the electrons, i.e., the same Lorentz factor as γ_{max} from Equation (7). For both terms, the correction factor to the power law coefficients is of the same form, e.g. for the emissivity j_ν,

$$j_\nu = j_{pl} \times \exp\left(\frac{-\nu}{Y\,\nu_c\,\sin^2\theta\,\gamma_{cutoff}^2}\right), \tag{17}$$

where j_{pl} is the power law coefficient determined by (7), $\nu_c = \frac{e\,B}{2\pi\,m_e\,c}$, the cyclotron resonance frequency, and Y is a coefficient to be determined.

By using the quasi-analytic model for the nonthermal j_ν, we are able to determine what the coefficient Y should be. Solving for Y we find that

$$Y = \frac{-\nu}{\nu_c \sin^2\theta\, \gamma_{cutoff}^2 \log(\frac{j_\nu}{j_{pl}})}. \tag{18}$$

By calculating a few coefficients for j_ν and j_{pl}, we can begin to determine Y for various: ν, B and θ. The same results can be obtained for the absorptivity coefficient, α_ν, by following the same procedure. These results are shown in Figure 4.

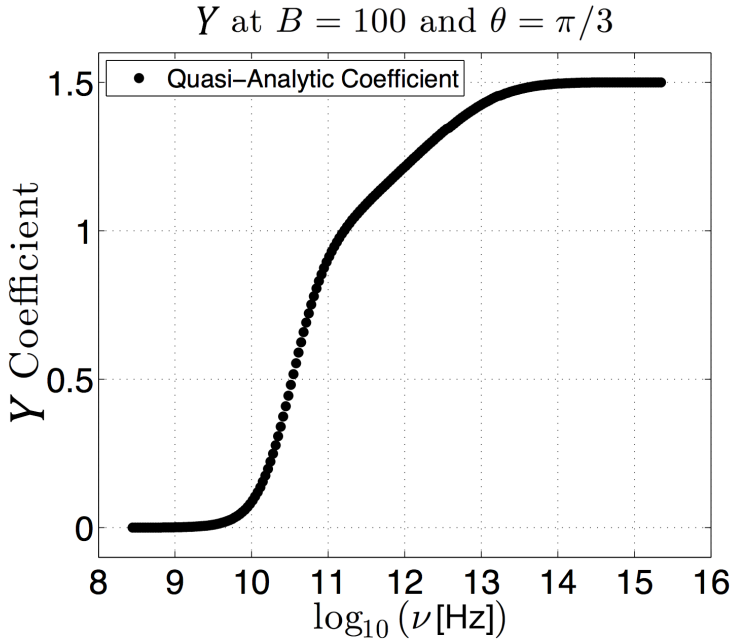

Figure 4: The results for solving for the Y coefficient at various frequencies. Each data point is calculated from a quasi-analytic method, which is highly computationally intensive. Note how the result asymptotes to 1.5 at higher frequencies.

3.4 Nonthermal implementation: spectrum

Prior to finding the approximate fitting formula, modeling an electron distribution function having a nonthermal component using a power law model to an unending tail in the spectrum. While power law implementation was able to model the emission from the infrared region, it over predicted emissions at higher frequencies.

Therefore, the spectra produced were not representative of what the synchrotron emission actually contributes. With the power law approximate fitting formula to the quasi-analytic coefficients, we can produce spectra using high accuracy relativity fast.

Several parameters of the power law implementation can be tuned to adjust the emission in the infrared region. Unique to the nonthermal component is the power law index of the distribution and the fraction of energy in the nonthermal component. A power law index of 2.6 and a ratio of 45:100 of nonthermal to thermal energy seem to produce some of the best fitting of simulated data to the observational data.

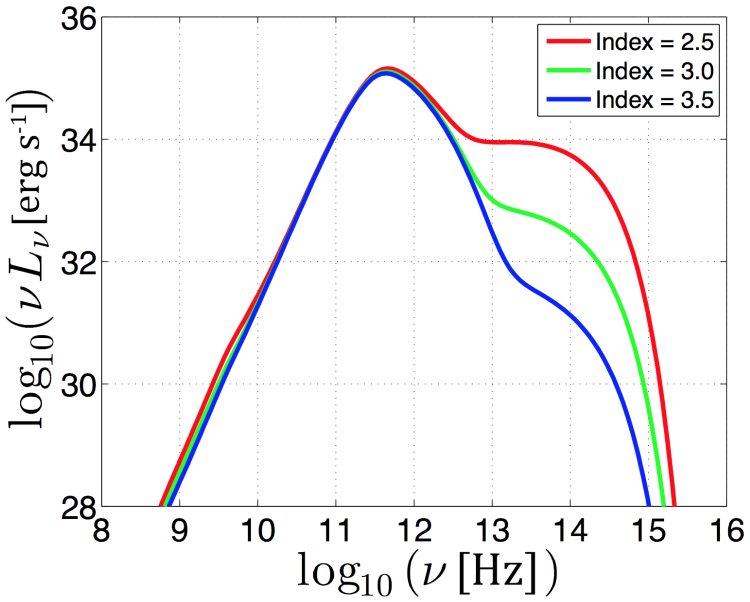

Figure 5: Shown are the spectra for three different power law indices using the approximate fitting formula implementation. Preliminarily results seem to to point to a power law index of 2.6 to account for observational data.

3.5 Nonthermal implementation: light curves

The simulations can also be used to observe the emission at a given frequency over some duration of time, rather than a specific time over a range of frequencies. Observing the emission at a given frequency over a period of time produces light curves. These light curves can be compared with the observational data taken from telescopes such as the Keck Telescope, which produced a 600–minute light curve of Sgr

A* in the near-infrared bands. Tuning our simulation to the parameters at which Keck observed the black hole, we can attempt to reproduce the light curve.

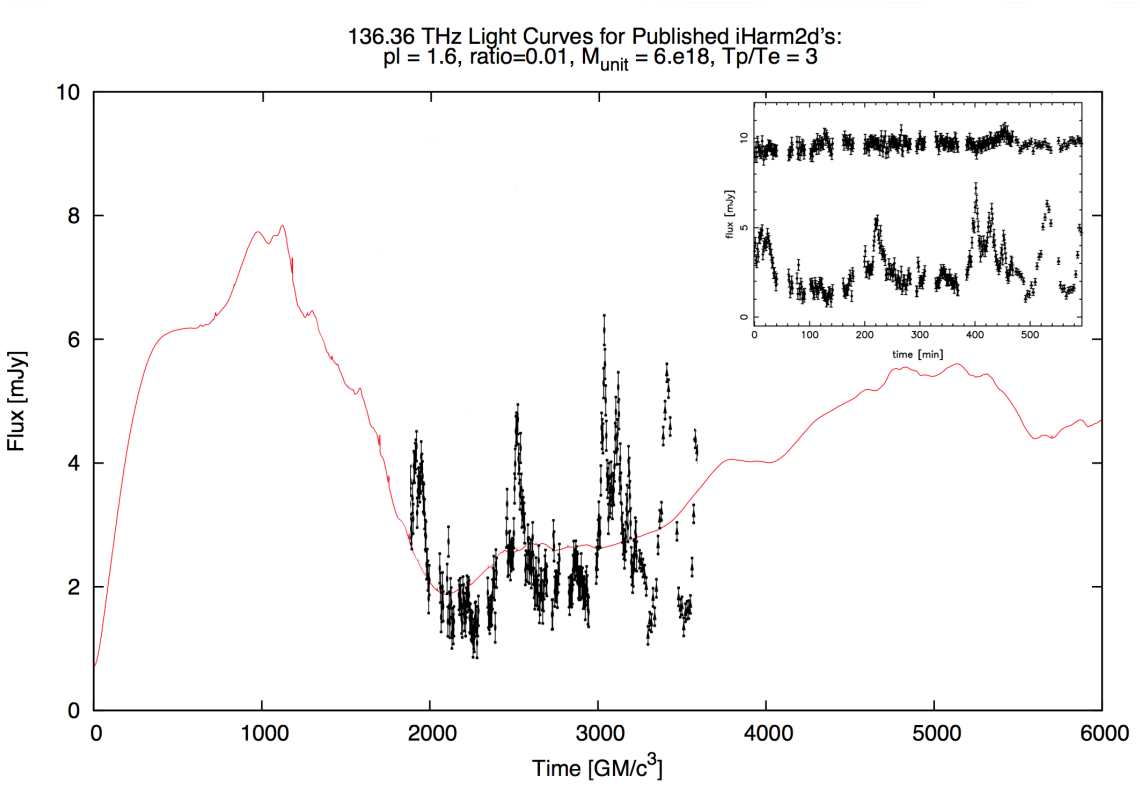

Figure 6: A light curve produced by ibothros2d at 136.36 THz is shown in red, black points represent data from the Keck Telescope of Sgr A* [9]. The duration of the simulated light curve is 6000 M, or 2,216 minutes, and Keck observations lasted 600 minutes. The insert shows the data collected from Keck of Sgr A*, the bottom curve is shows Sgr A*'s variation while the top curve is a nearby star with constant flux.

4 DISCUSSION

4.1 Agreement between ibothros2d and observations

Sgr A* is currently thought to be the closest supermassive black hole with respect to Earth; and the black hole subtending the largest portion of our sky. There exist other observational candidates, which could be used to test our model, i.e. Messier

87; however, given currently technological limitations, Sgr A* will be the first black hole candidate to be resolved. Therefore, the primary importance of these results is the ability to account for Sgr A*'s nonthermal emission from the infrared region. The emission from the infrared spectrum of Sgr A* is widely believed to be the result of a nonthermal component, given that the emission is highly polarized.

Our model uses calculations based on a nonthermal component in the electron distribution in the accretion flow. From our nonthermal implementation in ibothros2d, we find that the observational infrared data may be recovered. The model provides two free parameters which can be used to tune the spectral index and flux in the infrared region. Preliminarily, the best fit for the two parameters, the power law index, p, and nonthermal-to-thermal energy ratio, η, are $p = 2.6$ and $\eta = 0.10$. With these parameters and appropriate modeling, we can produce spectra which look very similar to observations.

The light curve produced by ibothros2d with the nonthermal implementation is also of the correct order of flux from the observational data. Observations done by the Keck telescope have shown that the flux is somewhere in the 4–6 mJy range [9]. However, the model currently does not have any implementations to explain the variation Sgr A*. Resolving the variation in a 2D seems unlikely, given the simplification to an axis symmetric model.

4.2 Light curve data selection

The light curves produced by ibothros2d, used to compare with the Keck observations have had several erroneous points removed from the presented data. Currently, it appears that the dump files produced from iHARM2D sporadically produces the erroneous simulated points. The corresponding dump files to these erroneous points are are producing an excess amount of flux on the order of 10^{20} greater than expected; however, the majority of the dumps appear correct and appear in the presented results. Further work is required to resolve the issue of the few erroneous data files, possibly caused by numerical cutoff conditions in the code.

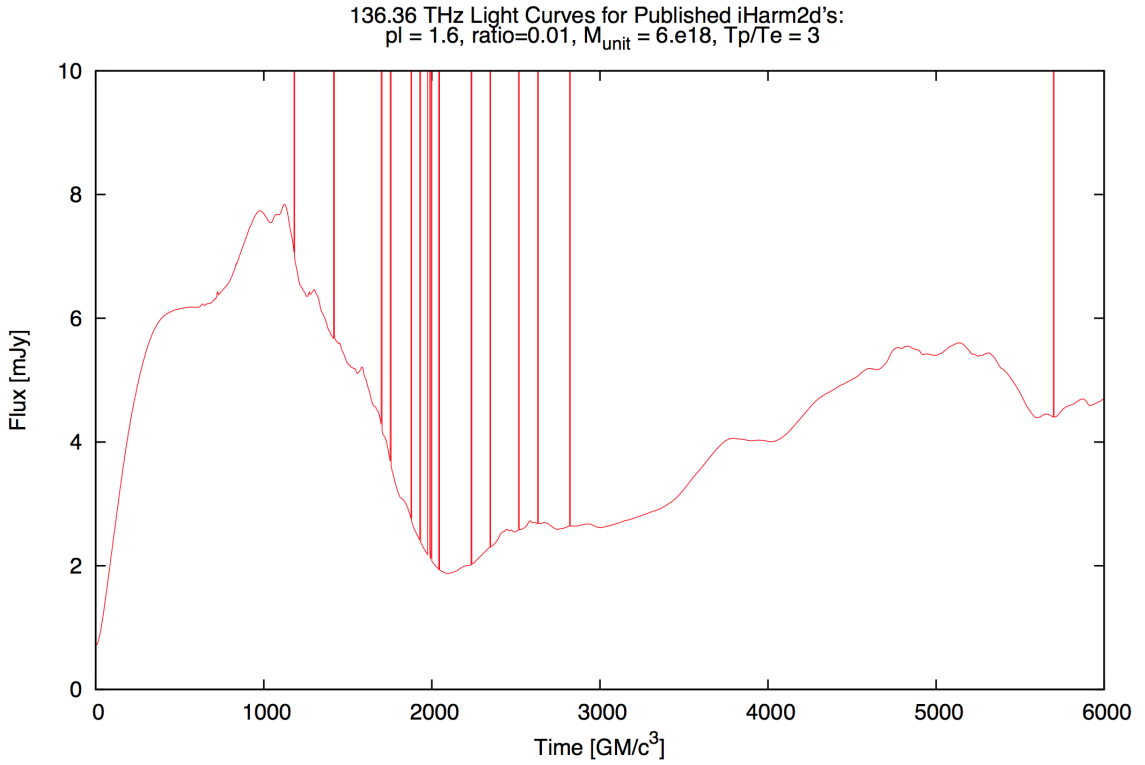

Figure 7: A light curve produced by ibothros2d at 136.36 THz is shown in red, the duration of the simulated light curve is 6000 M. The shown light curve is the same from from Figure 6, before simulated data is revoked. We note the spikes in the light curve go past our axis bounds by twenty orders of magnitude.

4.3 Infrared emission from other sources

Other processes, not taken into account in this model, are capable of producing infrared emission besides synchrotron radiation. Compton scattering is one such possibility as a source of infrared emission. Previous models have used Compton up scattering to explain the infrared emission, and emission at higher frequencies [3]; however, we have good reason to believe Compton scattering is not dominating the infrared emission around Sgr A*. The highly polarized emission from Sgr A* seen in observations is not compatible with Compton scattering. Compton scattering will produce highly unpolarized light, while synchrotron radiation will produce polarized light in its emission. The polarization of the emission is the best argument for why

the emission is from synchrotron radiation.

4.4 Approximations in model

Various approximations have been made to produce a numerically feasible simulation. The primary approximation to this work has been in the nonthermal emissivity and absorptivity coefficients. Quasi-analytic coefficients exist for both the emissivity and absorptivity; however, they are not numerically possible to simulate in a reasonable amount of time. Therefore, an approximate fitting formula has been used as discussed in Section 3.3.

HARM is a conservative scheme which updates the time steps by making sure that certain variables are conserved. These conserved variables are implicit to the simulations, and instead primitive variables are used explicitly in the calculations. The conversion from primitive to conserved variables has a closed analytic solution, however the conversion from conserved to primitive is not analytic [5]. Numerical methods are then used to solve two nonlinear differential equations.

5 CONCLUSIONS

Prior to beginning our work, models assumed a completely thermal component in the electron distribution, which could not fully account for the emission seen from Sgr A*. Adding a nonthermal component, modeled by a power law, to the distribution generated results more closely matching observational data. Initially, however, our nonthermal implementation produced excess emission at high frequencies not seen in observations. The reason for excess emission in our model was the over-estimation of the emissivity at frequencies the beyond infrared.

By working with a quasi-analytic model for the radiative transfer coefficients, i.e., emissivity and absorptivity, we determined an approximate fitting formula for these coefficients. This formula enables computational speedups, making it possible to run simulations of accreting black holes having a nonthermal component. These simulations are then compared with supermassive black hole systems, such as Sgr A*.

From our implementation of nonthermal electrons in accretion flows around supermassive black holes, we are able to account for infrared emission seen in observations of Sgr A*. Modeling the main component of the emission from synchrotron emission, we get a power law tail in the spectrum to account for the infrared emission missing from the thermal model. Our model allows for two parameters, i.e., the power law index and the energy ratio between the thermal and nonthermal populations, to find

a spectrum that can closely match the data. Preliminary tests suggest a power law index, p, of $2.6^{+0.2}_{-0.3}$ and an energy ratio, η, of $0.45^{+0.1}_{-0.25}$.

Using this model we can also produce light curves to match observational data, such as those taken by the Keck Telescope [9]. We find good agreement in the approximate magnitude of flux seen from Sgr A*; however, our model does not account for the rapid variation seen from Sgr A*. To obtain more variation in the flux, the first correction to the model would be moving into a 3D HARM simulation. However, even in 3D, our model would not account for flares seen in observations. Currently the physical processes responsible for these flares are unknown.

6 FUTURE WORK

6.1 Issues with iHARM2D

For simulation using GRMHD, all data of the disc were evolved using iHARM2D. The code iHARM2d was adapted from a 3D version of HARM, immediately prior to the beginning of the project. While producing spectra in ibothros2d from iHARM2D simulation data, the spectra appeared to have a few erroneous zones at random time steps. At higher resolutions in ibothros2d, we see a greater number of erroneous zones because of now resolving the individual zones. Resolving individual zones with erroneous data while other zone are correct suggests cutoff conditions for certain parameters, i.e., if electron temperature is below 0.3 set the electron temperature to 0.3, are causing the erroneous simulated data.

6.2 Better fit for Y

Currently the approximate fitting formula's coefficient Y, defined in Eq. (18), is taken as the asymptotic value in the high-frequency limit. However, this value breaks down in the low-frequency regime. While the low-frequency regime is not of interest to the infrared problem, further work can be done to find a better fit to the quasi-analytically calculated radiative transfer coefficients.

6.3 Tracking hot spots

Discovering orbits close to the innermost stable circular orbit (ISCO) of a super-massive black hole would provide a wealth of information about the black hole. An observationally exciting prospect would be a telescope having sufficiently high resolution to resolve any orbits close to the ISCO of Sgr A*. One possible ISCO candidate

would be the centriod of the synchrotron emission, called the hot spot. Current work being done on our model would enable predictions about the orbit of the hot spot.

6.4 Generation of nonthermal particles

Currently the process responsible for the generation of the nonthermal particles in black holes and various other astronomical objects is unknown. This process could involve first-order and second-order Fermi processes. Possible processes include shocks, magnetic reconnections, and flow shear [10]. Simulating these processes may lead to some insight about which process produces nonthermal electrons consistent with observations.

7 ACKNOWLEDGMENTS

This material is based upon work supported by the National Science Foundation under Grant No. 0709246. Any opinions, findings, and conclusions or recommendations expressed in this material are those of the author and do not necessarily reflect the views of the National Science Foundation. I am grateful to Dr. Charles Gammie, who was the advising professor on all of the work discussed. He provided the insight and resources that made the project possible. I am also grateful to Scott Luedtke, with whom I have been working with closely, Alex Stec, and Eric Petersen.

References

[1] P.K. Leung, C.F. Gammie, and S.C. Noble, *Numerical Calculation of Magnetobremsstrahlung Emission and Absorption Coefficients*. ApJ, **737**, 21, 2011.

[2] S. Markoff, H. Falcke, F. Yuan, P.L. Biermann, *Numerical Calculation of Magnetobremsstrahlung Emission and Absorption Coefficients*. A&A, **379**, 13, 2001.

[3] J.C. Dolence, C.F. Gammie, M. Mościbrodzka, P.K. Leung, *grmonty: A Monte Carlo Code for Relativistic Radiative Transport*. ApJS, **184**, 387, 2009.

[4] C.F. Gammie, J.C. McKinney, and G. Tòth, *HARM: A Numerical Scheme for General Relativistic Magnetohydrodynamics*. ApJ, **589**, 444, 2003.

[5] S.C. Noble, C.F. Gammie, J.C. McKinley, and D.L. Zanna, *Primitive Variable Solvers for Conservative General Relativistic Magnetohydrodynamics*. ApJ, **641**, 626, 2006.

[6] F. Özel, D. Psaltis, and R. Narayan, *Hybrid Thermal-Nonthermal Synchrotron Emission from Hot Accretion Flows*. ApJ, **541**, 234, 2000.

[7] C.F. Gammie and R. Popham, *Advection-dominated Accretion Flows in the Kerr Metric. I. Basic Equations*. ApJ, **498**, 313, 1998.

[8] J. Dexter, E. Agol, P.C. Fragile, and J.C. McKinney, *The Submillimeter Bump in Sgr A* from Relativistic MHD Simulations*. ApJ, **717**, 1092, 2010.

[9] L. Meyer, T. Do, A. Ghez, M. R. Morris, G. Witzel, A. Eckart, G. Bélanger, and R. Schödel, *A 600 Minute Near-infrared Light Curve of Sagittarius A**. ApJ, **688**, 17, 2008.

[10] M. Böttcher, D.E. Harris and H. Krawczynski, *Relativistic Jets from Active Galactic Nuclei*, 1st Ed. (WileyVCH, Weinheim, Germany, 2012), pp. 244-293.